Paper Submission Status

Paper Number: 2067

Paper Title: MULTI-MODAL/TEMPORAL GRAPH FUSION FOR CHANGE DETECTION IN MULTI-SPECTRAL IMAGES

Initial Submission Time Stamp: 10/18/2019 5:06:27 PM

Revised Submission Time Stamp: 10/21/2019 10:57:20 AM

Current Server Time: 12/5/2019 8:04:12 AM

Request Paper Withdraw: Click Here

Submission Topic

Code	Category	Topic
5.5.1	Image, Video, and Multidimensional Signal Processing	[IVARS] Image & Video Analysis, Synthesis, and Retrieval::[ARS-ANL] Image and Video Analysis
10.14	Sensor Array and Multichannel Signal Processing	[SAM-SENS] Multi-sensor remote sensing of the environment::

Status of Submission

Status	Item	Result
INCOMPLETE	Copyright Form	Copyright form not received. If you have recently sent your copyright form, please allow at least 14 days for processing.
COMPLETE	Paper Upload	Document has been uploaded.
COMPLETE	Paper Inspection	Document passed inspection.
IN PROGRESS	Technical Committee Review	Document is under review. No action is required by you at this time.
PENDING	Final Paper Upload	Document inspection pending review results.
PENDING	Final Paper Inspection	Document inspection pending final paper upload.
Paper Status		
PENDING	The paper status is pending outcome of the paper review.	

Active Papers

Current Submitted Paper : Download Date: 10/18/2019 5:28:35 PM

For questions about this page, or for technical support, contact icassp2020@cmsworkshops.com.

MULTI-MODAL/TEMPORAL GRAPH FUSION FOR CHANGE DETECTION IN MULTI-SPECTRAL IMAGES

David Alejandro Jimenez-Sierra† *Hernán Darío Benítez-Restrepo*† *Hernán Darío Vargas-Cardona*†
Jocelyn Chanussot⋆

† Pontificia Universidad Javeriana Cali
Departamento de Electrónica y Ciencias de la Computación
{davidjimenez, hbenitez, hernan.vargas}@javerianacali.edu.co
⋆ Grenoble Images Parole Signals Automatique Laboratory (GIPSA-Lab)
Grenoble Institute of Technology
jocelyn.chanussot@gipsa-lab.grenoble-inp.fr

ABSTRACT

This paper addresses semi-supervised change detection by proposing a framework of data fusion based on graph theory techniques. The proposed framework aims at: 1) The generation of a multi-modal/temporal pixel based graph, by the fusion of intra-graphs of each modality/temporal data; 2) the use of Nyström extension for obtaining the eigenvalues and eigenvectors of the fused graph and the selection of the final change map. We validated our approach in two real cases of remote sensing according to both qualitative and quantitative analyses. The results show that the fusion of temporal data based on graphs detects changes in remote sensing images with high accuracy in percentage with respect to missed alarms($\mathbf{4.8504}$), false alarms ($\mathbf{0.3120}$), precision ($\mathbf{0.9029}$), recall ($\mathbf{0.9515}$), cohen's kappa ($\mathbf{0.9242}$) and overall error ($\mathbf{0.4463}$), outperforming in most of these metrics the state of the art methods for change detection.

***Index Terms*—** Change detection, data fusion, graph, multi-modal, multi-spectral, multi-temporal, remote sensing.

1. INTRODUCTION

Change detection (CD) refers to the task of analyzing images acquired over an area of interest at different times, which allows to quantify the magnitude of a natural disaster (i.e flooding) or changes generated by human activities. This analysis provides fundamental data for environmental protection, sustainable development, and maintenance of ecological balance [1, 2]. One of the most known source of data for change detection are the Multi-spectral (MS) images that contain information from both spatial and spectral domain (i.e. Landsat series of satellites). Giving two or more co-registered images, pixel based approaches carry out change detection by probabilistic thresholding and machine learning methods [3, 4]. Even thought threshold methods are efficient and useful, they are sensitive to MS image noise and require a high accuracy in the estimation of the difference image probabilistic distribution. These issues make threshold methods prone to artifacts in the final change map [5–9]. Machine learning approaches divide into two categories: classification and clustering. Classification methods require a multitemporal reference, which is difficult to extract from the raw data. Therefore, these methods are not a practical solution [10]. Clustering techniques [11–15] are affected by parameters initialization, what may generate local minima in the learning stage. In addition, the intrinsic brightness distortion in MS images yields inaccurate change maps [4].

In order to reduce the effect of intra-class small variability and artifacts presented in MS images, we proposed a graph-based data fusion approach applied to CD. Our contribution is the extension of the graph-based model developed in [16]. In this case, we use the mutual information for extracting the relevant eigenvector that captures the change map. We validate our approach in two real cases: i) a flooding, and ii) a fire incident. Results show that our model reduces the effects of artifacts in the final change map, and it achieves low rates of false alarms in comparison to probabilistic threshold methods ([5–7]).

2. GRAPH BASED DATA FUSION

2.1. Graph

A graph is a non linear structural representation of data, defined by $G = (V, E)$, where G is the graph, V is a set of nodes, and E refers to the arcs or edges that explain the directed or undirected relationship between nodes. The edges have associated a weight $w_{i,j}$, that quantifies how strong is the relation between nodes. The common measure used for each weight is a Gaussian kernel [17]:

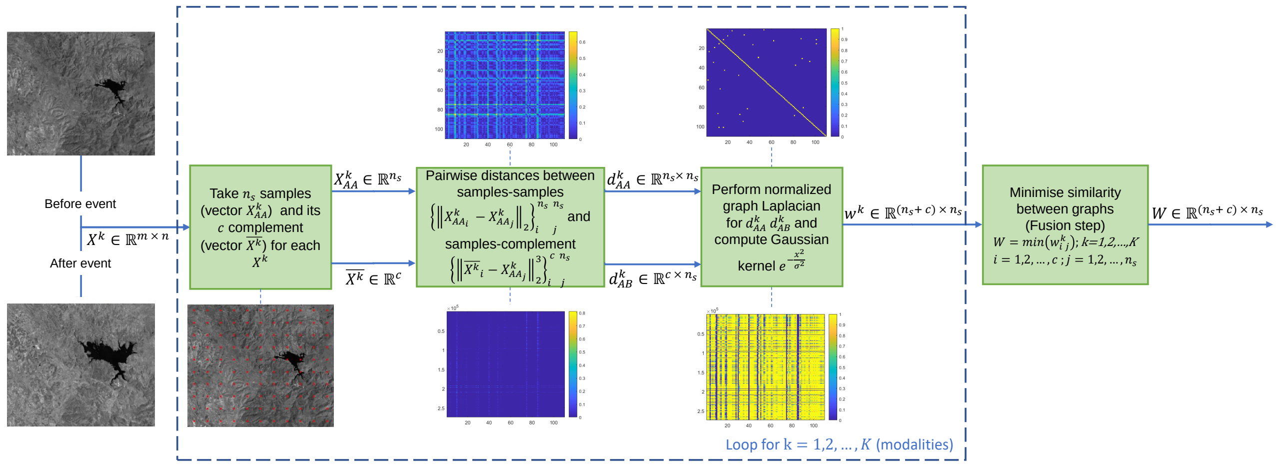

Fig. 1. Flow chart of multi-modal graph.

$$w_{i,j} = \exp\left(-\frac{d(V_i, V_j)^2}{\sigma^2}\right)$$

2.2. Multi-modal/temporal graph (MMT-G)

Based on the methodology introduced in [16], where a node is understood as a modality (i.e. image from different bands or times, also a mix of both) and it is assumed that all of the modalities are co-registered, the fusion of multi-modal/temporal data is carried out by the procedure described in Figure 1, where the dashed line goes through all modalities of interest and the output corresponds to the intra-modal normalized adjacency matrix $\mathbf{w}^k$ ($\mathbf{D}^{-\frac{1}{2}}\mathbf{W}\mathbf{D}^{-\frac{1}{2}}$ [18]). Taking into account that the goal of the fusion step is to capture the unique information given by each modality. In other words, it is to maximize the distance between nodes (i.e. the node that preserves more information) or to minimize the similarity between nodes. This is given by:

$$\mathbf{W} = min(w^k_{i,j}), \text{with } k = 1, 2, \ldots K,$$

where the super-index k denotes the modality, $w_{i,j}$ represents the weight of the node for each modality ($i = 1, 2, \ldots, c; j = 1, 2, \ldots, n_s$) and K is the number of modalities.

3. APPLICATION OF MMT-G FOR CHANGE DETECTION

3.1. Nyström extension

Given the high number of pixels in a MS image, the computational cost of calculating the full matrix $\mathbf{W} \in \mathbb{R}^{N \times N}$ is extremely high (i.e an image with size 1280×960 is equivalent to $N = 1228800$). Therefore, an approximation of this matrix is computed through the Nyström extension [18]:

$$\mathbf{W} = \begin{bmatrix} \mathbf{A} & \mathbf{B} \\ \mathbf{B}^\top & \mathbf{C} \end{bmatrix},$$

where $\mathbf{A} \in \mathbb{R}^{n_s \times n_s}$, $\mathbf{B} \in \mathbb{R}^{n_s \times (N-n_s)}$ and $\mathbf{C} \in \mathbb{R}^{(N-n_s)\times(N-n_s)}$. This method approximates $\mathbf{C}$ by using n_s samples from the N data ($n_s \ll N$). Thus, the eigenvectors of the matrix $\mathbf{W}$, can be spanned by eigenvalues and eigenvectors of $\mathbf{A}$. Solving the diagonalization of $\mathbf{A}$ (eigenvalues λ and eigenvectors $\mathbf{U}$: $\mathbf{A} = \mathbf{U}^\top\mathbf{\Lambda}\mathbf{U}$), the eigenvectors of $\mathbf{W}$ can be spanned by $\hat{\mathbf{U}} = \left[\mathbf{U}; \mathbf{B}^\top\mathbf{U}\mathbf{\Lambda}^{-1}\right]^\top$. Since the approximated eigenvectors $\hat{\mathbf{U}}$ are not orthogonal, as explained in [18], to obtain orthogonal eigenvectors it is defined $\mathbf{S} = \mathbf{A} + \mathbf{A}^{-\frac{1}{2}}\mathbf{B}\mathbf{B}^\top\mathbf{A}^{-\frac{1}{2}}$.Then, by diagonalization of $\mathbf{S}$ ($\mathbf{S} = \mathbf{U_s}\mathbf{\Lambda_s}\mathbf{U_s}$) the final approximated eigenvectors of W are given by:

$$\hat{\mathbf{U}} = \begin{bmatrix} \mathbf{A} \\ \mathbf{B}^\top\mathbf{A}^{-\frac{1}{2}} \end{bmatrix} \mathbf{U_s}\mathbf{\Lambda_s}^{-\frac{1}{2}}.$$

3.2. Change detection scheme based on multi-modal/multi-temporal graph

To get the change map from the multi-modal/temporal graph (section 2), we apply the scheme detailed in Figure 2. Here, the purpose is to attain the best match that reflects the change produced by any source. To do this, we use the eigenvectors from the MMT-G as descriptors of the change. Nevertheless, the number of eigenvectors is equal to the samples taken from modalities. Hence, we estimate the mutual information to identify the relevant eigenvector that captures the global change.

The output in Figure 2 is a vector that contains the mutual information between the prior knowledge (difference image) and the change map generated by the eigenvectors of the MMT-G. It is important to mention that an image given by an eigenvector of the MMT-G (I_{u_i}) must be rearranged,

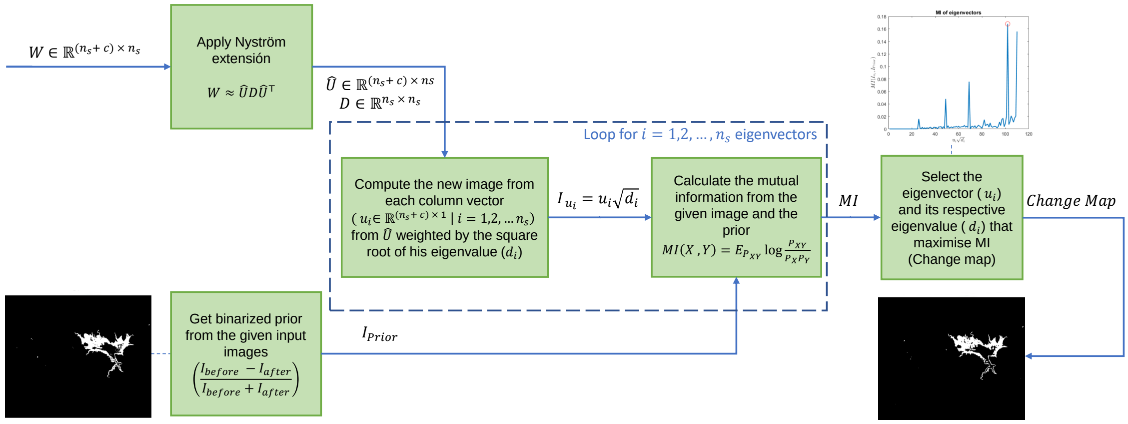

Fig. 2. Flow chart for change detection.

because the samples are taken from different regions of the image. In Nyström extension the approximated vector comes from a matrix with the form $[\mathbf{A} \quad \mathbf{B}]^{\top}$. However, the real locations of $\mathbf{A}$ and $\mathbf{B}$ correspond to the same location were the samples were taken from the image (samples and complement respectively). Finally the change map detected is the eigen-image (I_{u_i}) that maximizes the mutual information.

4. EXPERIMENTAL RESULTS AND DISCUSSION

4.1. Databases

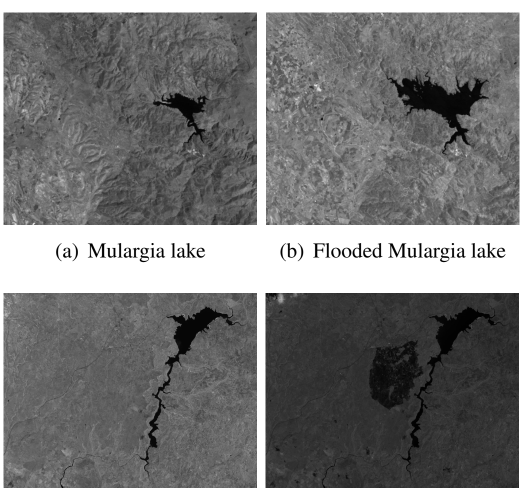

(a) Mulargia lake (b) Flooded Mulargia lake

(c) Omodeo lake (d) Fire near Omodeo lake

Fig. 3. Satellite images from the NIR band for the flood event (*Dataset A*) and from the red band for fire event (*Dataset B*).

Dataset A: Images (Figure 3 (a-b)) were acquired by the Thematic Mapper (TM) MS sensor of the Landsat-5 satellite. The scene represents an area including Lake Mulargia (Sardinia Island, Italy). The images consist of 573×479 pixels. The dates of acquisition were September 1995 (before event) and July 1996 (after event).

Dataset B: Images (Figure 3 (c-d)) were acquired by the Operational Land Image MS sensor of the Landsat-8 satellite. The area includes Lake Omodeo and a portion of Tirso River (Sardinia Island, Italy). The images consist of 965×742 pixels. The dates of acquisition were July 25, 2013 (before event) and August 10, 2013 (after event).

4.2. Experimental set-up

We compare the proposed MMT-G with state of the art methods: Rayleigh-Rice (rR) [6], Rayleigh-Rayleigh-Rice (rrR) [7], and the classical Kittler–Illingsworth (KI) [5]. We evaluate relevant metrics in change detection such as: missed alarms (MA), false alarms (FA), precision (P), recall (R), Cohen's kappa (K) and overall error (OE).

The number of samples (n_s) was fixed at 92 and the standard deviations (σ) for the kernels of the intra-modal adjacency were $\sigma^1_{lake} = 2.5299 \times 10^{-10}$, $\sigma^2_{lake} = 1.5561 \times 10^{-10}$, $\sigma^1_{fire} = 2.793 \times 10^{-11}$ and $\sigma^2_{fire} = 1.6533 \times 10^{-10}$, where the superscripts 1, 2 stands for pre and post event respectively. We set these values through cross-validation using $MatLab^{®}2017a$.[1]

Table 1. Model Performance for dataset A.

Method	MA (%)	FA (%)	P	R	K	OE (%)
KI [5]	10.2425	1.0490	0.7229	0.8975	0.7941	1.3211
rR-EM [6]	5.7245	4.0147	0.4173	0.9427	0.5605	4.0653
rrR-EM [7]	10.1440	1.0637	0.7203	0.8985	0.7928	1.3324
MMT-G	**4.8504**	**0.3120**	**0.9029**	**0.9515**	**0.9242**	**0.4463**

Table 1 shows the results for dataset A. We observe our approach outperforms the comparison methods for all metrics. Similarly, Table 2 tabulates the outcomes for dataset B.

[1]To ensure the reproducibility of the proposed method, the code is publicly available at: `https://github.com/DavidJimenezS/MMT-G-for-Change-detection.git`

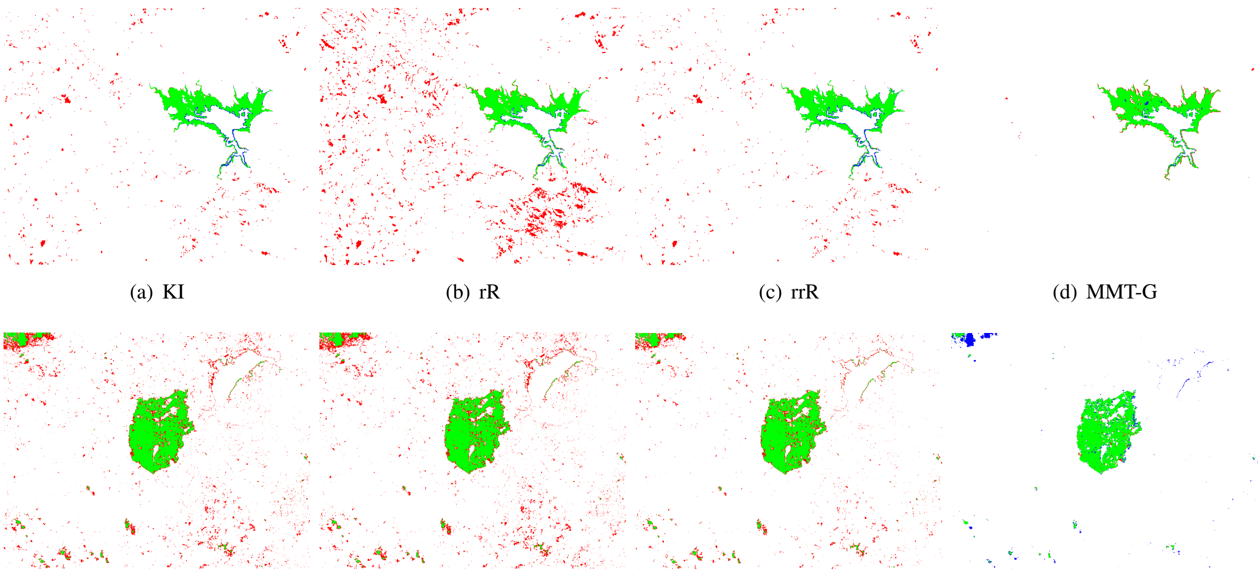

(a) KI (b) rR (c) rrR (d) MMT-G

(e) KI (f) rR (g) rrR (h) MMT-G

Fig. 4. Change map detected with respect to missed alarms (MA), false alarms (FA) and corrrect changed pixels (C).

Table 2. Model Performance of dataset B.

Method	MA (%)	FA(%)	P	R	K	OE (%)
KI [5]	0	3.4291	0.5903	1	0.7262	3.2676
rR-EM [6]	0.0029	3.7382	0.5693	0.9999	0.7080	3.5623
rrR-EM [7]	0.0029	2.1449	0.6973	0.9999	0.8112	2.0440
MMT-G	14.4217	**0.1226**	**0.9718**	0.8557	**0.9059**	**0.7960**

Although, **KI** method achieves a perfect score for MA and recall (R), the **MMT-G** outperforms the state-of-the-art methods in FA, P, K and OE.

Also, Figure 4 shows the behavior of each method in terms of MA (blue points), FA (red points) and correct changed pixels (green points). These results are remarkable because we can see that probabilistic methods have a considerable number of FA in both datasets. Conversely, the **MMT-G** deals well with this issue. FA is mostly generated by the nearly similar intensity of pixels between real changes regions and effects produced by the reflectance (i.e. weather variations, cloud density, daylight differences when the image was captured). The **MMT-G** has some limitations. Firstly, for dataset A (see subfigure 4 (d)), we can observe that border of the change map is mainly composed by red points (FA). This is due to the neigboring pixels of the border have a similar intensity. Also, for dataset B (see figure 4 (h)), the **MMT-G** is unable to detect minor changes in the edge of lake Omodeo and the artifact located in the left-superior corner. For this reason, there are some missed alarms (MA) represented by the blue points.

Other aspect to be taken into account in the proposed model: (i) to decrease the dependence of the results with respect to the number of selected samples for the Nyström extension, (ii) to select an alternative metric instead of Euclidean distance (ED) to increase the difference between intensities in MS images and avoid raising the ED to the power three, (iii) to explore other kernel types.

5. CONCLUSIONS

In this paper, we introduced a change detection methodology (**MMT-G**) based on graphs data fusion. Our main contribution is a "semisupervised" framework, where we use the mutual information from eigenvectors of the multi-modal graph and the prior information (the difference image). Experimental results showed that **MMT-G** outperformed probabilistic threshold methods when we evaluated several metrics (MA, FA, R, P, K, OE) over two real cases of change detection in remote sensing images.

According to the previous results and analysis, we can establish the **MMT-G** is a promising and robust approach for detecting changes in remote sensing images.

Acknowledgments This work was funded by the OMICAS program: "Optimización Multiescala In-silico de Cultivos Agrícolas Sostenibles (Infraestructura y validación en Arroz y Caña de Azúcar)", sponsored within the Colombian Scientific Ecosystem by The WORLD BANK, COLCIENCIAS, ICETEX, the Colombian Ministry of Education and the Colombian Ministry of Industry and Turism under GRANT ID: FP44842-217-2018.

6. REFERENCES

[1] Mauro Dalla Mura, Saurabh Prasad, Fabio Pacifici, Paulo Gamba, Jocelyn Chanussot, and Jón Atli Benediktsson, "Challenges and opportunities of multimodality and data fusion in remote sensing," *Proceedings of the IEEE*, vol. 103, no. 9, pp. 1585–1601, 2015.

[2] Dana Lahat, Tülay Adali, and Christian Jutten, "Multimodal data fusion: an overview of methods, challenges, and prospects," *Proceedings of the IEEE*, vol. 103, no. 9, pp. 1449–1477, 2015.

[3] Amir Yavariabdi and Huseyin Kusetogullari, "Change detection in multispectral landsat images using multiobjective evolutionary algorithm," *IEEE Geoscience and Remote Sensing Letters*, vol. 14, no. 3, pp. 414–418, 2017.

[4] Mi Song, Yanfei Zhong, and Ailong Ma, "Change detection based on multi-feature clustering using differential evolution for landsat imagery," *Remote Sensing*, vol. 10, no. 10, pp. 1664, 2018.

[5] Josef Kittler and John Illingworth, "Minimum error thresholding," *Pattern recognition*, vol. 19, no. 1, pp. 41–47, 1986.

[6] Massimo Zanetti, Francesca Bovolo, and Lorenzo Bruzzone, "Rayleigh-rice mixture parameter estimation via em algorithm for change detection in multispectral images," *IEEE Transactions on Image Processing*, vol. 24, no. 12, pp. 5004–5016, 2015.

[7] Massimo Zanetti and Lorenzo Bruzzone, "A theoretical framework for change detection based on a compound multiclass statistical model of the difference image," *IEEE Transactions on Geoscience and Remote Sensing*, vol. 56, no. 2, pp. 1129–1143, 2017.

[8] Ammar Mian, Guillaume Ginolhac, Jean-Philippe Ovarlez, and Abdourrahmane Mahamane Atto, "New robust statistics for change detection in time series of multivariate sar images," *IEEE Transactions on Signal Processing*, vol. 67, no. 2, pp. 520–534, 2018.

[9] Redha Touati, Max Mignotte, and Mohamed Dahmane, "Multimodal change detection in remote sensing images using an unsupervised pixel pairwise based markov random field model," *IEEE Transactions on Image Processing*, 2019.

[10] Begüm Demir, Francesca Bovolo, and Lorenzo Bruzzone, "Classification of time series of multispectral images with limited training data," *IEEE Transactions on Image Processing*, vol. 22, no. 8, pp. 3219–3233, 2013.

[11] Ashish Ghosh, Niladri Shekhar Mishra, and Susmita Ghosh, "Fuzzy clustering algorithms for unsupervised change detection in remote sensing images," *Information Sciences*, vol. 181, no. 4, pp. 699–715, 2011.

[12] Turgay Celik, "Change detection in satellite images using a genetic algorithm approach," *IEEE Geoscience and Remote Sensing Letters*, vol. 7, no. 2, pp. 386–390, 2010.

[13] Maoguo Gong, Zhiqiang Zhou, and Jingjing Ma, "Change detection in synthetic aperture radar images based on image fusion and fuzzy clustering," *IEEE Transactions on Image Processing*, vol. 21, no. 4, pp. 2141–2151, 2011.

[14] Vladimir A Krylov, Gabriele Moser, Sebastiano B Serpico, and Josiane Zerubia, "False discovery rate approach to unsupervised image change detection," *IEEE Transactions on Image Processing*, vol. 25, no. 10, pp. 4704–4718, 2016.

[15] Zhunga Liu, Gang Li, Gregoire Mercier, You He, and Quan Pan, "Change detection in heterogenous remote sensing images via homogeneous pixel transformation," *IEEE Transactions on Image Processing*, vol. 27, no. 4, pp. 1822–1834, 2017.

[16] Geoffrey Iyer, Jocelyn Chanussot, and Andrea L Bertozzi, "A graph-based approach for feature extraction and segmentation of multimodal images," in *2017 IEEE International Conference on Image Processing (ICIP)*. IEEE, 2017, pp. 3320–3324.

[17] Rosa María Ménedez Parra Alfredo Caicedo Barrero, Graciela Wagner de García, "Introducción a la teoría de grafos," vol. 1, pp. 1–12. Elizcom s.a.s, 2010.

[18] Charless Fowlkes, Serge Belongie, Fan Chung, and Jitendra Malik, "Spectral grouping using the Nyström method," *IEEE Transactions on Pattern Analysis and Machine Intelligence*, vol. 26, no. 2, pp. 214–225, 2004.